

# Human Activity Classification Using MHI and MEI with SVM, KNN, and MLP Classifiers

Karthik Nagesh

College of Computing / Computer Science

Geargia Institute of Technology

Email: knagesh3@gatech.edu

[Source Code – Box Link](#)

**Abstract**—This paper presents a human activity recognition system that leverages Motion History Images (MHI) and Motion Energy Images (MEI) in combination with classical machine learning classifiers, including Support Vector Machines (SVM),  $k$ -Nearest Neighbors (KNN), and Multi-Layer Perceptrons (MLP). Using Hu moment descriptors extracted from the motion templates, we first evaluate how each classifier performs under a compact, low-dimensional representation of global motion shape. We then extend this representation by introducing a set of auxiliary motion features that capture temporal variation, spatial motion distribution, and localized activity intensity.

Through these refinements—together with calibrated motion thresholds and temporal decay parameters—the SVM classifier shows a substantial improvement in both validation and video-level accuracy, surpassing the performance of all baseline Hu-only models. The results demonstrate that simple engineered motion descriptors can meaningfully enhance the discriminative power of traditional temporal templates, while also motivating the exploration of richer feature representations, such as HOG or learned deep features, in future work.

## I. INTRODUCTION

Human activity recognition (HAR) plays an important role in applications such as surveillance, human–computer interaction, consumer devices, sports analytics, automotive safety, and healthcare monitoring. A central challenge is to represent human motion in a way that is compact, discriminative, and robust to variations in subjects, appearance, and viewpoint. Although deep learning approaches dominate modern HAR, classical motion-template methods remain attractive due to their interpretability and computational efficiency.

Motion History Images (MHI) and Motion Energy Images (MEI), introduced by Bobick and Davis [1], transform video sequences into static templates that summarize where motion occurs and how it evolves over time. Their simplicity and ability to encode coarse action dynamics have made them foundational in early action-recognition pipelines. To illustrate the diversity of actions considered in this work, representative frames for all six activity classes are shown in Figure 1

Once constructed, these templates support the extraction of global shape-based features. Hu moments provide a compact, invariant descriptor widely used in classical vision tasks [3]. More expressive local descriptors such as Histograms of Oriented Gradients (HOG) [4] capture fine spatial detail and highlight the trade-off between simplicity and representational richness—an important theme motivating this work.



Fig. 1: Representative frames for all six actions in the dataset

This paper evaluates an MHI/MEI-based action-recognition system using three classical classifiers: Support Vector Machines (SVM) [12],  $k$ -Nearest Neighbors (KNN), and a lightweight Multi-Layer Perceptron (MLP). All models are trained on Hu-moment descriptors, enabling a controlled comparison under a low-dimensional, globally defined feature representation.

The system pipeline includes preprocessing, motion-template construction, feature extraction, classifier training, and evaluation. Our results highlight both the strengths and limitations of Hu-moment features: they effectively capture coarse motion patterns but struggle with fine distinctions among similar actions [1]. These findings, together with advances in spatiotemporal feature learning [10], motivate future exploration of richer descriptors such as HOG, trajectory-based features, or learned CNN representations.

## II. RELATED WORK

### A. Motion Energy Images (MEI)

Motion Energy Images (MEI) [1], capture the spatial extent of motion over the most recent  $\tau$  frames. MEI is defined as a binary motion template:

$$E_\tau(x, y, t) = \begin{cases} 1, & \text{if motion occurs in } [t - \tau, t], \\ 0, & \text{otherwise.} \end{cases} \quad (1)$$

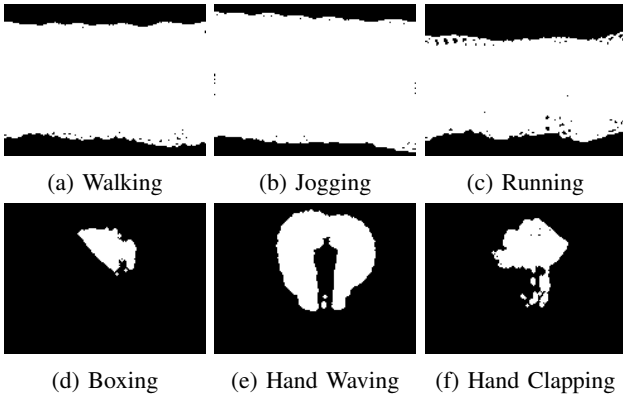


Fig. 2: MEI templates for six actions

In this formulation, motion is detected through thresholded frame differencing, following the classical temporal-template approach [1]:

$$D(x, y, t) = \begin{cases} 1, & |I(x, y, t) - I(x, y, t-1)| > \theta, \\ 0, & \text{otherwise.} \end{cases} \quad (2)$$

*MEI Templates Across Six Actions:* Figure 2 shows MEI templates for six representative actions (walking, jogging, running, boxing, hand waving, and hand clapping). These binary silhouettes highlight the overall spatial footprint of motion accumulated over time, revealing differences in limb usage, displacement, and body posture across actions. For walking, jogging, and running, the MEIs appear as large white blobs because the actor moves left-to-right and back across the frame. Since MEI represents the union of all motion regions over time, any pixel touched during these actions becomes active, resulting in a broad motion band.

#### B. Motion History Images (MHI)

Motion History Images (MHI) encode the recency of motion by assigning larger intensity values to pixels where motion has occurred more recently:

$$M_\tau(x, y, t) = \begin{cases} \tau, & \text{if } B_\tau(x, y) = 1 \\ \max\{0, M_\tau(x, y, t-1) - 1, 0\}, & \text{if } B_\tau(x, y) = 0. \end{cases} \quad (3)$$

*Binary Motion Mask and Background Subtraction:* Both MEI and MHI use a binary motion mask derived from frame differencing:

$$B_\tau(x, y, t) = \begin{cases} 1, & |I_\tau(x, y) - I_{\tau-1}(x, y)| \geq \theta, \\ 0, & \text{otherwise.} \end{cases} \quad (4)$$

This mask identifies regions of movement by comparing consecutive frames. Light smoothing can be applied before differencing to suppress noise. Where MEI simply accumulates these binary masks, MHI applies temporal decay, producing a gradient that reflects \*how motion evolves over time\*.

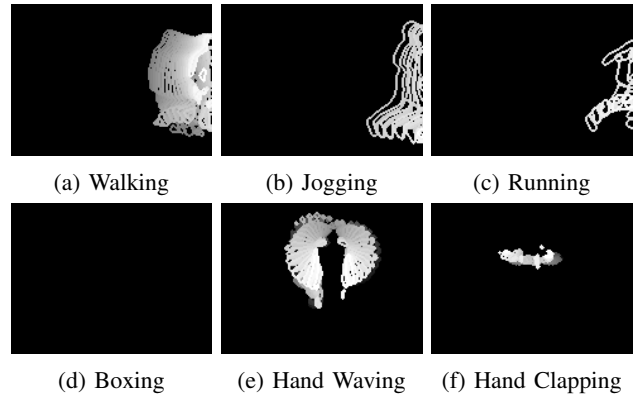


Fig. 3: MHI templates for six actions.

#### C. Preliminaries: Image Moments and Normalized Central Moments

The Hu moment invariants used in this work are derived from standard image moment definitions [7]. These expressions describe how spatial information in an image is aggregated and normalized to achieve invariance to translation, rotation, and scale.

*Raw Image Moments:* Given an image intensity function  $I(x, y)$ , the  $(p, q)$ -th raw moment is defined as:

$$M_{pq} = \sum_x \sum_y x^p y^q I(x, y). \quad (5)$$

*Centroid of the Image:* The centroid  $(\bar{x}, \bar{y})$  is computed from the first-order raw moments:

$$\bar{x} = \frac{M_{10}}{M_{00}}, \quad \bar{y} = \frac{M_{01}}{M_{00}}. \quad (6)$$

*Central Moments:* Translation-invariant central moments are computed by shifting coordinates relative to the centroid:

$$\mu_{pq} = \sum_x \sum_y (x - \bar{x})^p (y - \bar{y})^q I(x, y). \quad (7)$$

*Normalized Central Moments:* Scale-invariant normalized central moments are obtained as:

$$\nu_{pq} = \frac{\mu_{pq}}{\mu_{00}^{1 + \frac{p+q}{2}}}. \quad (8)$$

These normalized moments form the basis for the Hu invariant descriptors used in the next subsection, allowing activity templates such as MHI and MEI to be represented using compact shape measures that are invariant to geometric transformations.

*MHI Templates Across Six Actions:* Figure 3 displays MHI templates for the same six actions. Unlike MEI—which only shows where movement occurred—MHI distinguishes between recent and older motion. Brighter areas correspond to more recent movement, making MHI a richer temporal descriptor.

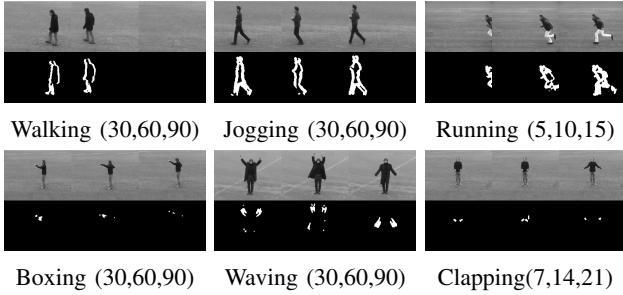


Fig. 4: Binary motion evidence at different frames is indicated in braces for each action sequence.

#### Evidence: Binary Motion Detection Across Time

To demonstrate the foundation upon which MEI and MHI are constructed, Figure 4 presents binary motion masks extracted at three different time instants[1]. Each image is produced by thresholding pixel differences between consecutive frames, highlighting only the regions where motion occurred at that moment.

These examples show how different actions produce distinct temporal patterns: locomotion actions such as walking and jogging generate smoother, periodic silhouettes, whereas high-frequency actions like boxing or hand clapping produce denser, rapidly changing motion regions.

### III. CLASSIFICATION

This work evaluates three supervised classifiers—SVM, KNN, and MLP—using Hu moment descriptors extracted from MHI and MEI templates in the human action dataset. The dataset was divided into a **75% training, 15% validation, and 15% test split**. This ensures that all models are evaluated consistently while preventing overlap between subjects across splits. Because all models operate on the same compact, low-dimensional feature representation, the comparison highlights differences in how each classifier handles these constraints rather than differences arising from the features themselves.

#### A. Dataset Split Overview

To provide a clear view of how the video samples were distributed across the three subsets, Figure 5 presents a simple histogram-style visualization showing the number of videos assigned to training, validation, and testing.

This visualization emphasizes that the majority of samples contribute to model training, while dedicated validation and test subsets enable unbiased hyperparameter tuning and final performance assessment.

#### B. k-Nearest Neighbors (KNN)

KNN assigns labels based on the nearest samples in the Hu-moment feature space. Since it makes no assumptions about how classes should be separated, its performance is strongly influenced by the structure and noise inherent in the descriptors. Earlier studies have noted that KNN is particularly prone to overfitting in low-dimensional spaces where class clusters lie close together [2]. This behavior is reflected in our

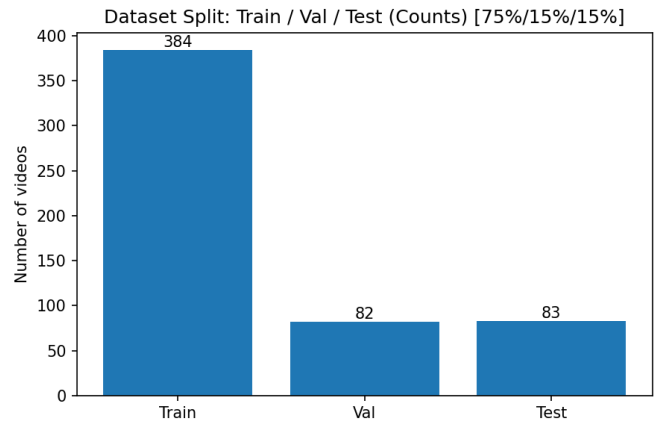


Fig. 5: Dataset split visualization showing the number of videos allocated to the 75/15/15 train–validation–test partitions.

dataset as well: actions involving whole-body motion, such as walking, jogging, and running, produce Hu features that overlap significantly. As a result, KNN performs extremely well on the training data but struggles to generalize to new sequences, where differences in subjects, motion style, lighting, or camera instability cause small variations that shift samples across class boundaries.

#### C. Support Vector Machine (SVM)

SVM seeks a decision boundary that maximizes the margin between action classes in the Hu-moment feature space. Because the descriptors are compact and the classes partially overlap, margin-based separation is generally more robust than distance-based approaches. This aligns with earlier work demonstrating the effectiveness of SVMs in such settings [12]. In our dataset, actions like walking, jogging, and running share similar global motion patterns, which makes them difficult to separate cleanly. Even so, the SVM maintains relatively stable generalization performance, handling variations in subject appearance, execution speed, and recording conditions better than KNN.

#### D. Multi-Layer Perceptron (MLP)

The MLP introduces a simple neural network capable of modeling nonlinear relationships in the feature space. Although neural networks typically excel with rich, high-dimensional inputs [13], the MLP here receives only a 14-dimensional Hu descriptor per frame. Because Hu moments capture only coarse global structure, the network’s expressive capacity is not fully utilized. As a result, the MLP behaves similarly to the SVM: it improves slightly on some classes but is ultimately limited by the information available in the Hu features. This reinforces the idea that the main challenge lies in the representation rather than in the choice of classifier.

Overall, the comparison indicates that when using compact global descriptors such as Hu moments, classifier performance

is largely constrained by feature limitations rather than model complexity.

#### IV. ANALYSIS

To compare the behavior of the three classifiers, we consolidate the main performance metrics in Table I. This provides a unified view of training, validation, test, and video-level accuracy across SVM, KNN, and MLP when all three models are trained using Hu moments extracted from MHI and MEI. The table is reported in the Results section; here we focus on interpreting the trends it reveals.

##### A. Key Observations

*Limited discriminative power of Hu features.*: Hu moments provide compact global shape descriptors, but they offer limited ability to separate visually similar activities, a limitation noted in prior template-based action recognition research [1]. Because all classifiers rely on the same low-dimensional representation, their performance is inherently constrained by the descriptive power of Hu moments.

##### B. Effect of Subject and Scene Variability

The dataset includes substantial intra-class variability: different subjects perform the same action with variations in body shape, clothing, motion style, and execution speed. Similar challenges in human action recognition datasets have been documented in earlier evaluations [6]. Because Hu moment features extracted from MHI/MEI templates encode only coarse global motion shape, they are not expressive enough to disentangle these variations. Consequently, actions such as walking, jogging, and running—already visually similar—become even harder to discriminate when performed by different individuals under different conditions.

*KNN exhibits pronounced overfitting.*: KNN achieves nearly perfect training accuracy but shows a substantial drop in validation and test performance. This behavior is consistent with classical observations that KNN is highly sensitive to small variations when classes are not well separated in feature space [2]. In our case, overlapping Hu moment descriptors cause unstable nearest-neighbor relationships, limiting generalization.

*SVM shows more stable generalization.*: SVM avoids the extreme overfitting observed in KNN and produces more balanced performance across training and test sets. Prior work has shown that SVMs generalize effectively in low-dimensional settings with overlapping features by maximizing the decision margin [12]. Nevertheless, their accuracy remains constrained by the limited separability inherent in Hu-based representations.

*MLP performs comparably but is feature-limited.*: Although MLPs can model nonlinear relationships, their performance does not substantially exceed that of SVM when trained on simple descriptors. Similar effects have been reported in earlier neural-network-based action analysis, where limited features restrict the benefits of nonlinear models. Because the MLP receives only 14 global shape features, its expressive capacity is underutilized.

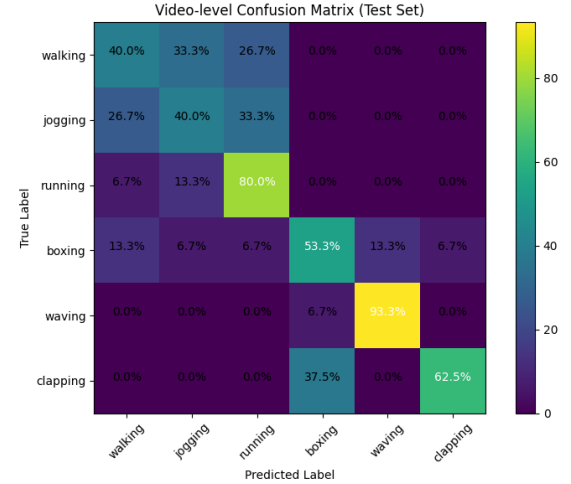


Fig. 6: SVM classifier using Hu moment features.

TABLE I: Performance results for all classifiers using Hu moment features.

Classifier	Train	Val	Test	Video Acc.
SVM (Hu)	0.764	0.577	0.514	0.627
KNN (Hu)	1.000	0.476	0.453	0.651
MLP (Hu)	0.748	0.553	0.512	0.627

*Upper-bound limitations.*: Across all three classifiers, accuracy remains below higher performance thresholds due to factors commonly cited in template-based action-recognition systems: (i) compression of temporal information in silhouette templates, (ii) similarity among certain actions (walking, jogging, running), and (iii) subject-level variability [1], [6]. These factors contribute to classification ambiguity that is not fully resolved by Hu-based descriptors.

Taken together, the analysis highlights that while classifier choice influences generalization behavior, the primary performance limitations stem from the restricted descriptive capacity of Hu moments.

##### C. Confusion Matrix Visualization

To further illustrate how each classifier distributes predictions across activity classes, Figures 6, 7, and 8 present the confusion matrices for SVM, KNN, and MLP. These matrices visualize class-specific behavior, including which actions are consistently recognized and where misclassifications occur.

## V. RESULTS

This section presents the quantitative outcomes obtained from the three classifier configurations evaluated in this work. To avoid redundancy, we summarize all measured performance metrics in a single consolidated table (Table I). These values include training, validation, test, and video-level accuracy for each classifier trained on Hu moment descriptors extracted from MHI and MEI templates.

For completeness, confusion matrices for each classifier configuration were generated and are included as figures in

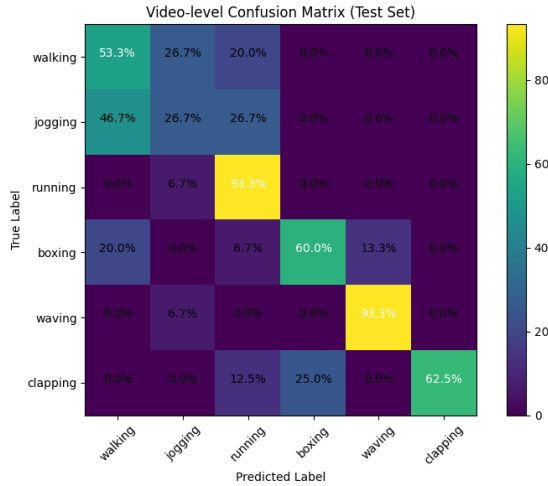


Fig. 7: KNN classifier using Hu moment features.

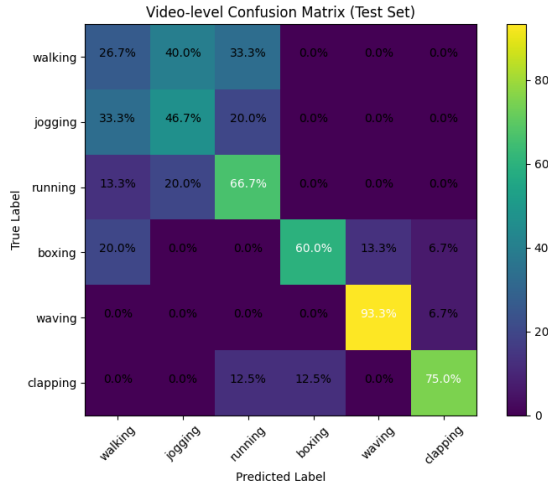


Fig. 8: MLP classifier using Hu moment features.

the results section. These matrices illustrate the distribution of predicted labels across classes but are not interpreted here, as further discussion is provided in the Analysis section.

In addition to accuracy values, the trained pipelines for each experiment (SVM, KNN, and MLP) were saved for reproducibility. The corresponding feature matrix dimensions reflect the use of Hu moment descriptors, resulting in a 14-dimensional feature vector for every video frame.

## VI. IMPROVEMENTS

After evaluating SVM, KNN, and MLP on Hu moment features, SVM consistently offered the most stable performance. It was therefore selected as the primary candidate for improvement. The refinements described below build on a baseline Hu-only model that had already been tuned to a reasonable level before additional enhancements were introduced.

### A. Feature Expansion: From 14D Hu Moments to a 20D Motion Descriptor

The original feature representation consisted of 14 values: the seven Hu moments extracted from the MHI and the seven Hu moments extracted from the MEI. While compact and effective for capturing global shape, this 14D descriptor omits several important characteristics of human motion, such as intensity, localization, and temporal variability. To address this limitation, six additional motion descriptors were introduced, expanding the feature vector from 14 to 20 dimensions.

This expansion strengthens the representation in three key ways:

- **Capturing motion magnitude:** Aggregated motion-pixel counts provide a direct measure of how much motion occurs in a frame, helping distinguish high-intensity actions (running, boxing) from lower-intensity ones (walking).
- **Encoding temporal dynamics:** Features such as the frame-to-frame change in the MHI and the short-term standard deviation of motion quantify how stable, periodic, or bursty an action is—properties not encoded by Hu moments.
- **Preserving spatial structure:** Lower-body motion, central-region motion, and central-to-side ratios describe how motion is distributed across the frame. These cues differentiate actions with similar overall silhouettes but different spatial emphasis (e.g., running vs. boxing).

By augmenting the Hu feature space with these lightweight descriptors, the SVM operates in a richer but still low-dimensional space where classes are more separable. This expansion from 14D to 20D significantly enhances the model’s ability to discriminate between actions with subtle motion differences, as validated by improved validation and video-level accuracy.

### B. Parameter Calibration

Several parameters controlling MHI/MEI construction were adjusted:

- $\tau$  (decay): balanced temporal smoothing vs. motion persistence,
- $\theta$  (threshold): reduced noise in motion masks,
- $k\_size$  (Gaussian blur): stabilized differencing,
- reset frequency: prevented MHI saturation.

These refinements produced cleaner templates and more reliable features, helping the SVM separate visually similar actions such as walking, jogging, and running.

### C. Performance Comparison

Table II summarizes the improvement over the baseline Hu-only SVM. The largest gain appears in video-level accuracy, rising from approximately 0.63 to over 0.80.

### D. Confusion Matrix Evidence

Figure 9 shows the confusion matrix of the improved model. Compared to earlier runs, the diagonal is noticeably stronger and confusions between locomotion classes are substantially

TABLE II: Comparison of SVM performance before and after adding auxiliary motion features.

Model	Train	Val	Test	Video Acc.
Baseline SVM (Hu-only)	0.764	0.577	0.514	0.627
Improved SVM (Hu + extra feats)	0.939	0.682	0.622	0.807

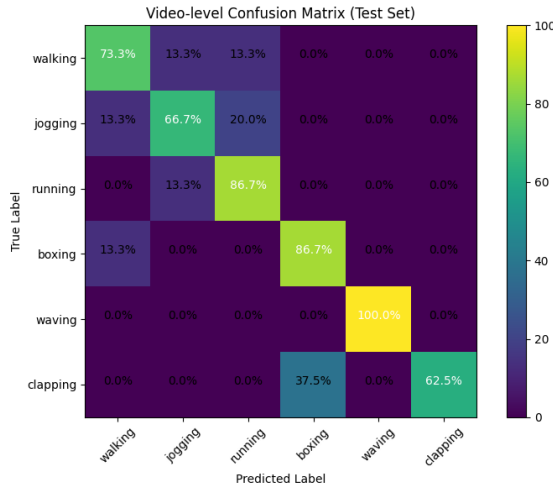


Fig. 9: Confusion matrix of the improved SVM classifier using Hu moments plus auxiliary motion features. Strengthened diagonal entries reflect clearer class separation.

reduced. This reflects the added discriminative value of the auxiliary motion descriptors.

#### E. Summary

Overall, the improvements result from:

- a richer feature set augmenting Hu moments,
- calibrated motion-template parameters,
- cleaner and more stable MHI/MEI representations.

These changes enabled the SVM to outperform all earlier Hu-based models while preserving interpretability and computational simplicity.

## VII. FUTURE WORK

The results obtained using Hu moments across SVM, KNN, and MLP suggest that the main limitation lies in the expressiveness of the features rather than the classifiers. Improving the quality of the descriptors is therefore the most promising direction for increasing recognition accuracy. Several focused extensions are outlined below.

#### A. Richer Spatial Descriptors: HOG Features

Hu moments capture only coarse global shape. Incorporating more expressive handcrafted descriptors such as Histograms of Oriented Gradients (HOG) could provide finer spatial detail and strengthen class separability. Since the existing MHI/MEI pipeline already supports gradient-based representations, HOG offers a natural next step for comparison and improvement.

#### B. Deep Feature Extraction Using CNNs

Convolutional neural networks learn high-level spatial representations directly from data and have demonstrated strong performance in action-recognition tasks [11]. Applying CNN-based feature extraction to MHI/MEI templates—or directly to raw video frames—may yield richer and more robust descriptors than handcrafted features, enabling the model to learn discriminative motion cues automatically.

#### C. Temporal Modeling Beyond Static Templates

MHI and MEI compress motion into a single static image, discarding temporal ordering. Future extensions could incorporate models that preserve sequence structure, such as LSTMs, GRUs, or temporal CNNs [14]. These approaches capture how motion evolves over time and may improve performance on actions where temporal progression is critical.

Overall, richer handcrafted descriptors, learned deep features, and explicit temporal modeling represent promising pathways for advancing the performance of template-based human activity recognition systems.

## VIII. REFERENCES

### REFERENCES

- [1] A. F. Bobick and J. W. Davis, “The recognition of human movement using temporal templates,” *IEEE Transactions on Pattern Analysis and Machine Intelligence*, vol. 23, no. 3, pp. 257–267, 2001.
- [2] T. M. Cover and P. E. Hart, “Nearest Neighbor Pattern Classification,” *IEEE Transactions on Information Theory*, vol. 13, no. 1, pp. 21–27, 1967.
- [3] H. Ming-Kuei, “Visual pattern recognition by moment invariants,” *IRE Transactions on Information Theory*, vol. 8, no. 2, pp. 179–187, 1962.
- [4] N. Dalal and B. Triggs, “Histograms of oriented gradients for human detection,” in *Proceedings of the IEEE Conference on Computer Vision and Pattern Recognition (CVPR)*, 2005, pp. 886–893.
- [5] B. Schölkopf and A. J. Smola, *Learning with Kernels*. MIT Press, 2002.
- [6] C. Schuldt, I. Laptev, and B. Caputo, “Recognizing human actions: A local SVM approach,” in *Proc. IEEE International Conference on Pattern Recognition (ICPR)*, 2004.
- [7] M.-K. Hu, “Visual pattern recognition by moment invariants,” *IRE Transactions on Information Theory*, vol. 8, no. 2, pp. 179–187, 1962.
- [8] A. Kläser, M. Marszalek, and C. Schmid, “A spatio-temporal descriptor based on 3D-gradients,” in *Proc. British Machine Vision Conference (BMVC)*, 2008.
- [9] W. Yang, Y. Wang, and G. Mori, “Evaluating temporal information in human action recognition,” in *Proc. IEEE International Conference on Computer Vision (ICCV)*, 2007.
- [10] A. Klaser, M. Marszalek, and C. Schmid, “A spatio-temporal descriptor based on 3D-gradients,” in *British Machine Vision Conference (BMVC)*, 2008.
- [11] K. Simonyan and A. Zisserman, “Two-stream convolutional networks for action recognition in videos,” in *Proc. Advances in Neural Information Processing Systems (NeurIPS)*, 2014.
- [12] C. Cortes and V. Vapnik, “Support-vector networks,” *Machine Learning*, vol. 20, pp. 273–297, 1995.
- [13] D. E. Rumelhart, G. E. Hinton, and R. J. Williams, “Learning representations by back-propagating errors,” *Nature*, vol. 323, pp. 533–536, 1986.
- [14] S. Ji, W. Xu, M. Yang, and K. Yu, “3D convolutional neural networks for human action recognition,” *IEEE Transactions on Pattern Analysis and Machine Intelligence*, vol. 35, no. 1, pp. 221–231, 2013.